



# Synergistic Cooperation between Two ClpB Isoforms in Aggregate Reactivation

Maria Nagy<sup>1</sup>, Izabela Guenther<sup>2</sup>, Vladimir Akoyev<sup>1</sup>,  
Micheal E. Barnett<sup>1</sup>, Maria I. Zavodszky<sup>3</sup>,  
Sabina Kedzierska-Mieszkowska<sup>2</sup> and Michal Zolkiewski<sup>1\*</sup>

<sup>1</sup>Department of Biochemistry,  
Kansas State University,  
141 Chalmers Hall, Manhattan,  
KS 66506, USA

<sup>2</sup>Department of Biochemistry,  
University of Gdansk,  
80-822 Gdansk, Poland

<sup>3</sup>Department of Biochemistry  
and Molecular Biology,  
Michigan State University,  
East Lansing, MI 48824, USA

Received 7 August 2009;  
received in revised form  
10 November 2009;  
accepted 25 November 2009  
Available online  
1 December 2009

Bacterial AAA<sup>+</sup> ATPase ClpB cooperates with DnaK during reactivation of aggregated proteins. The ClpB-mediated disaggregation is linked to translocation of polypeptides through the channel in the oligomeric ClpB. Two isoforms of ClpB are produced *in vivo*: the full-length ClpB95 and ClpB80, which does not contain the substrate-interacting N-terminal domain. The biological role of the truncated isoform ClpB80 is unknown. We found that resolubilization of aggregated proteins in *Escherichia coli* after heat shock and reactivation of aggregated proteins *in vitro* and *in vivo* occurred at higher rates in the presence of ClpB95 with ClpB80 than with ClpB95 or ClpB80 alone. Combined amounts of ClpB95 and ClpB80 bound to aggregated substrates were similar to the amounts of either ClpB95 or ClpB80 bound to the substrates in the absence of another isoform. The ATP hydrolysis rate of ClpB95 with ClpB80, which is linked to the rate of substrate translocation, was not higher than the rates measured for the isolated ClpB95 or ClpB80. We postulate that a reaction step that takes place after substrate binding to ClpB and precedes substrate translocation is rate-limiting during aggregate reactivation, and its efficiency is enhanced in the presence of both ClpB isoforms. Moreover, we found that ClpB95 and ClpB80 form hetero-oligomers, which are similar in size to the homo-oligomers of ClpB95 or ClpB80. Thus, the mechanism of functional cooperation of the two isoforms of ClpB may be linked to their heteroassociation. Our results suggest that the functionality of other AAA<sup>+</sup> ATPases may be also optimized by interaction and synergistic cooperation of their isoforms.

© 2009 Elsevier Ltd. All rights reserved.

**Keywords:** AAA<sup>+</sup> ATPase; ClpB; protein aggregation; molecular chaperone; heat shock

Edited by F. Schmid

## Introduction

Bacteria, yeast, and plants contain chaperone systems involving heat shock proteins from the Hsp100 and Hsp70 families that resolubilize and reactivate aggregated proteins.<sup>1–3</sup> Hsp100 chaper-

ones (bacterial ClpB and yeast Hsp104) belong to the AAA<sup>+</sup> (ATPases associated with various cellular activities) superfamily.<sup>4</sup> ClpB contains two AAA<sup>+</sup> ATP-binding sequence modules (D1 and D2) with an inserted coiled-coil domain and a distinct N-terminal domain connected to D1 with a flexible linker (see Fig. 1).<sup>5</sup> Like other AAA<sup>+</sup> ATPases, ClpB forms nucleotide-stabilized ring-shaped hexamers with a narrow channel at the center of the ring.<sup>6</sup> The ClpB hexamers are only transiently stable and undergo dynamic association–dissociation with subunit exchange.<sup>7</sup> The mechanism of protein disaggregation mediated by ClpB involves extraction of polypeptides from aggregated particles and their forced unfolding by translocation through the

\*Corresponding author. E-mail address: [michalz@ksu.edu](mailto:michalz@ksu.edu).

Present address: M. Nagy, Yale University School of Medicine and Howard Hughes Medical Institute, New Haven, CT 06510, USA.

Abbreviations used: G6PDH, glucose-6-phosphate dehydrogenase; MDH, malate dehydrogenase; EDTA, ethylenediaminetetraacetic acid.

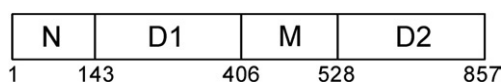


**Fig. 1.** Domain structure of ClpB. The diagram shows the structural domains of ClpB<sup>5</sup>: N-terminal domain (N), D1 AAA<sup>+</sup> module, middle coiled-coil domain (M), and D2 AAA<sup>+</sup> module. The residue numbers are given for *E. coli* ClpB.

channel in the hexameric ClpB.<sup>8</sup> The dynamic instability of ClpB hexamers prevents nonproductive trapping of the chaperone by resistant aggregates.<sup>7</sup> Selected substrates can be processed by ClpB alone,<sup>8,9</sup> but reactivation of strongly aggregated proteins requires cooperation between ClpB and DnaK/DnaJ/GrpE.<sup>2,8</sup> The mechanism of aggregate recognition by ClpB, the events preceding substrate translocation, and the role of the cochaperones remain poorly understood.

The ClpB transcript contains two translation initiation sites: the first one at the N-terminus of the N-terminal domain and the second one at the N-terminus of D1. Consequently, two isoforms of ClpB are produced *in vivo*: the full-length 95-kDa ClpB (ClpB95) and a truncated 80-kDa isoform that lacks the N-terminal domain (ClpB80).<sup>10</sup> The *in vivo* molar ratio of chromosomally encoded ClpB80 and ClpB95 varies between 2/5 and 1/2, depending on the severity of heat shock.<sup>11</sup>

The N-terminal domain of ClpB95, which is missing in ClpB80 (see Fig. 1), contributes to aggregate binding affinity and becomes essential for binding to large protein aggregates.<sup>12</sup> Consequently, ClpB80 is less efficient than ClpB95 in reactivating some strongly aggregated substrates *in vitro*.<sup>12</sup> *In vivo*, a deficiency of ClpB80 in supporting bacterial thermotolerance manifests itself in the background of a defective DnaK, which promotes strong protein aggregation.<sup>13</sup> One might ask: If ClpB80 is a lower-efficiency chaperone compared to ClpB95, then why has the alternative translation initiation site in the ClpB gene not been eliminated during evolution? What role does the truncated ClpB isoform play in the cellular chaperone machinery?

The optimal survival of *Escherichia coli* during heat shock is achieved when both ClpB95 and ClpB80 are produced.<sup>11</sup> This result suggests that the two isoforms of ClpB may cooperate in producing a highly efficient chaperone system. Indeed, it has been found that purified ClpB95 and ClpB80 interact in the presence of ATP.<sup>14</sup> It has not been determined, however, if the interaction occurs between homohexameric ClpB95 and ClpB80, or between monomeric isoforms with the formation of heterohexamers. The functional significance of the heteroassociation of the two ClpB isoforms has not been explored either. In this work, we discovered that ClpB95 and ClpB80 form heterohexamers, and that the chaperone activity of ClpB95 with ClpB80 is superior to that of either ClpB95 or ClpB80.

## Results

### Functional interaction of ClpB95 with ClpB80 boosts the aggregate reactivation potential

The initial rate of reactivation of strongly aggregated glucose-6-phosphate dehydrogenase (G6PDH) by the bichaperone system (ClpB + DnaK/DnaJ/GrpE) was significantly faster in the presence of ClpB95 than in the presence of ClpB80 (Fig. 2a), consistent with a weaker binding of ClpB80 to large G6PDH aggregates.<sup>12</sup> Unexpectedly, we observed a strong stimulation of chaperone activity (up to a 3-fold increase in the G6PDH reactivation rate) when both ClpB95 and ClpB80 were used in the reactivation assay (at a constant total ClpB concentration), with the highest G6PDH reactivation rate for the molar fraction of ClpB80  $f_{\text{ClpB80}}$  being 0.5 (Fig. 2a and c). Another substrate, thermally aggregated malate dehydrogenase (MDH), was reactivated with a similar rate by ClpB80 or ClpB95 (Fig. 2b), indicating that the N-terminal domain of ClpB is not apparently involved in the reactivation of MDH. However, the reactivation rate of aggregated MDH again increased in the presence of both ClpB isoforms and reached a maximum for  $f_{\text{ClpB80}} = 0.5$  (Fig. 2b and c). These results demonstrate that mixtures of ClpB95 and ClpB80 work more efficiently as aggregate-reactivating chaperones than either ClpB95 or ClpB80 alone. The reactivation rates achieved with ClpB95/ClpB80 were higher than the rates expected with ClpB isoforms working independently (Fig. 2c, broken lines). The highest ClpB activity in these *in vitro* assays is observed for  $f_{\text{ClpB80}} = 0.5$ , but a strong enhancement of activity is also evident for  $f_{\text{ClpB80}} \sim 0.3$ , which is found *in vivo*.<sup>11</sup>

It has been shown that both ClpB isoforms are required for optimal survival of *E. coli* under heat shock.<sup>11</sup> We asked whether the synergy between ClpB95 and ClpB80 might lead to an enhanced rate of clearing aggregates in heat-stressed bacteria. We monitored the formation and removal of thermally aggregated proteins<sup>15</sup> in *clpB*-null *E. coli* strain transformed with plasmids encoding ClpB95 with ClpB80, ClpB95 alone, or ClpB80 alone (see Materials and Methods). Heat shock induction in the strain carrying pClpB95/ClpB80 resulted in production of excess ClpB95 over ClpB80 (see Fig. 3a). No ClpB80 was produced in cells transformed with pClpB95, and no ClpB95 was produced in cells transformed with pClpB80. Both ClpB95 and ClpB80 were found in the fraction of thermally aggregated proteins isolated from cells transformed with pClpB95/ClpB80 (Fig. 3a), and the ClpB80/ClpB95 ratio that copurified with the aggregates was approximately 1/2, as determined with Scion Image software (data not shown), agreeing with the ClpB80/ClpB95 ratio found in chromosomal expression.<sup>11</sup>

The amount of thermally aggregated proteins isolated from *E. coli* after 15 min of heat shock was ~33% of the total insoluble cellular fraction and did not depend on whether and which ClpB isoform

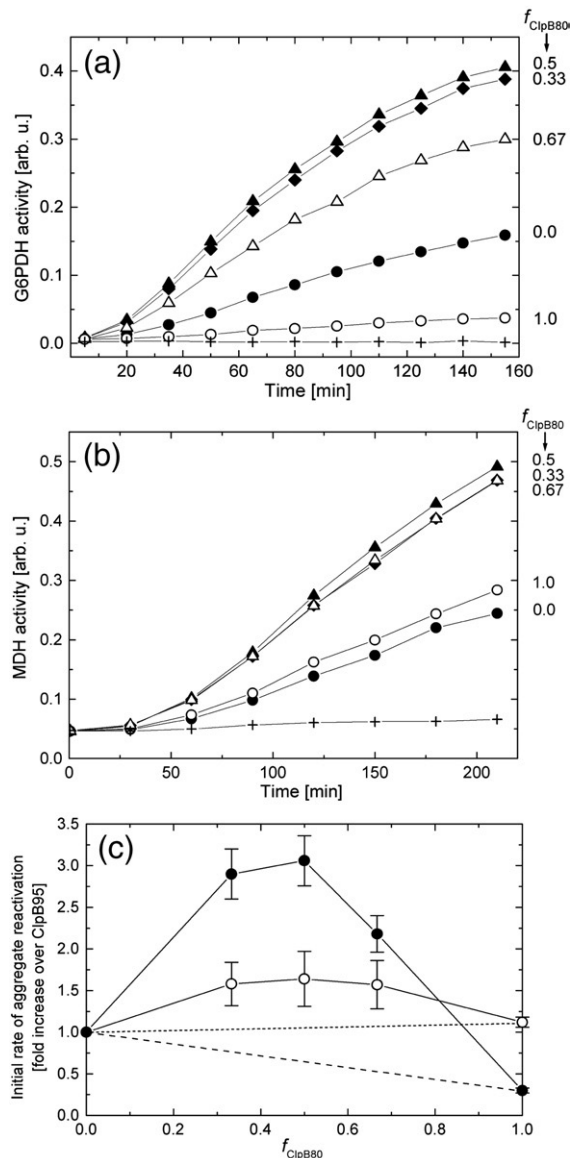


**Fig. 2.** Reactivation of aggregated G6PDH (a) or MDH (b) in the presence of the ClpB/DnaK bichaperone system. The aggregates were diluted into buffer A (G6PDH) or buffer B (MDH) with 6 mM ATP containing either no chaperone (crosses), 1  $\mu$ M DnaK, 1  $\mu$ M DnaJ, 0.5  $\mu$ M GrpE (KJE) with 1.5  $\mu$ M ClpB95 (filled circles), KJE with 1.5  $\mu$ M ClpB80 (open circles), KJE with 1  $\mu$ M ClpB95 and 0.5  $\mu$ M ClpB80 (diamonds), KJE with 0.75  $\mu$ M ClpB95 and 0.75  $\mu$ M ClpB80 (filled triangles), or KJE with 0.5  $\mu$ M ClpB95 and 1  $\mu$ M ClpB80 (open triangles). After incubation at 30 °C for the indicated time, aliquots were withdrawn, and G6PDH or MDH activity was measured. The molar fraction of ClpB80:  $f_{ClpB80} = [ClpB80] / ([ClpB95] + [ClpB80])$  is indicated for each data set. Representative data from three independent experiments are shown. (c) G6PDH activity after 35 min of reactivation (filled symbols) and MDH activity after 60 min (open symbols) are shown as the function of  $f_{ClpB80}$ . Average changes over the activities observed with ClpB95 are plotted together with standard deviations from three experiments. Broken lines correspond to the predicted results if no synergy between ClpB95 and ClpB80 occurred in G6PDH reactivation (long dash) or MDH reactivation (short dash).

was produced (data not shown). This result confirms that ClpB does not protect cellular proteins from thermal aggregation.<sup>16</sup> As expected, the removal of aggregated proteins occurred more efficiently with either ClpB95 or ClpB80 than in the absence of ClpB (Fig. 3b), but the rate of aggregate clearance was suboptimal with either isoform. Only in the presence of both ClpB95 and ClpB80 did *E. coli* achieve an efficient removal of aggregated proteins. Notably, the rates of aggregate clearing achieved with ClpB95 and ClpB80 separately do not add up to the rate achieved with ClpB95/ClpB80, which demonstrates again a synergistic cooperation between the two isoforms.

In a different assay, we monitored the reactivation of specific enzymes *in vivo* after their thermal inactivation in the same bacterial strains as those used in Fig. 3. Bacterial luciferase (Fig. 4a) or firefly luciferase (Fig. 4b) was reactivated in *E. coli* after heat shock in the presence, but not in the absence, of ClpB. In agreement with the experiments described above, ClpB95 with ClpB80 produced the most efficient reactivation of either enzyme. The rates and yields of reactivation in the presence of ClpB95/ClpB80 were again higher than could be accounted for by the activities of ClpB95 and ClpB80 acting separately. Altogether, our results demonstrate that two isoforms of ClpB synergistically cooperate *in vitro* and *in vivo* and produce a highly efficient aggregate-reactivating chaperone system.

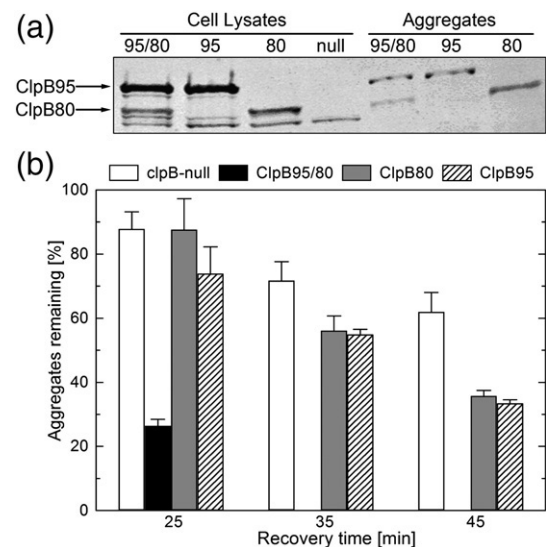


**Fig. 3.** Resolubilization of aggregated proteins in *E. coli* after heat shock. (a) Immunodetection of ClpB in bacterial lysates and the isolated aggregated fraction in the strains producing ClpB95 and/or ClpB80 after 15 min of heat shock. The lysate from the *clpB*-null strain is shown as control. (b) The protein content of the aggregated fraction was measured during the recovery of *E. coli* cells at 37 °C after a 15-min heat treatment at 45 °C. The data are shown for the *clpB*-null strain (white bars) and the strains producing ClpB95 and ClpB80 (black bars), ClpB80 (gray bars), or ClpB95 (hatched bars). Average values from three experiments are shown with standard deviations.



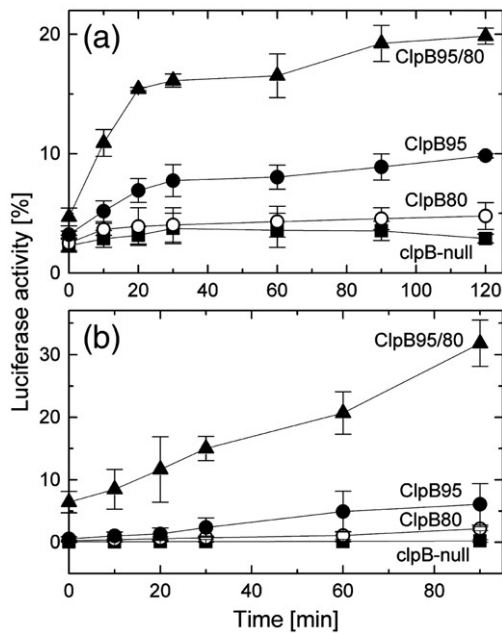


**Fig. 4.** Reactivation of heat-inactivated luciferases in *E. coli* cells. *E. coli* cultures producing bacterial luciferase (a) or firefly luciferase (b) were exposed to 25 min or 15 min of heat shock, respectively, at 45 °C. Luciferase activity was measured during cell recovery at 30 °C. The data are shown for the *clpB*-null strain (squares) and the strains producing ClpB95 and ClpB80 (triangles), ClpB80 (open circles), or ClpB95 (filled circles) (see ClpB expression patterns in Fig. 3a). The mean values from four independent experiments are shown with standard deviations.

### Superior chaperone activity of ClpB95/ClpB80 is not linked to either substrate binding efficiency or ATP hydrolysis rate

We asked whether the population of ClpB95/ClpB80 bound to aggregated substrates is higher than that of ClpB95 and ClpB80 separately, which could account for the increased rate of aggregate reactivation in the presence of both ClpB isoforms (see Fig. 2). We used the same conditions as those in Fig. 2, except that wild-type ClpB95 and ClpB80 were replaced with their Walker-B mutants that bind but do not hydrolyze ATP: ClpB95(E279Q/E678Q) and ClpB80(E279Q/E678Q). In the presence of ATP, these ClpB variants are “frozen” in the high-affinity conformation and bind stably to their substrates.<sup>17</sup> After incubating the aggregated G6PDH or MDH with the chaperones, we separated the aggregates from soluble proteins using filtration and resolved proteins bound to the aggregates with SDS-PAGE (Fig. 5). As has been shown before, the capture of ClpB during filtration of large aggregates is strictly ATP-dependent, validating this assay for the study of ClpB–substrate interactions.<sup>18</sup>

Only trace amounts of ClpB are retained on filters in the absence of aggregated substrates with native G6PDH or MDH (Fig. 5, lanes 9 and 10). As expected, ClpB80 binds weakly to aggregated G6PDH, but binds more strongly to aggregated

MDH (lane 5, compare Fig. 2a and b). However, band density analysis of Fig. 5 and repeated experiments failed to detect a significant increase in the combined amount of ClpB95 together with ClpB80 bound to the aggregates, as compared to separated ClpB95 and ClpB80 (Fig. 5, lane 7 versus lanes 3 and 5; data not shown). Analogous results were obtained when gel-filtration chromatography was used to detect ClpB bound to aggregates of different sizes (data not shown). Moreover, the lack of the excess aggregate binding capability of ClpB95/ClpB80 was observed in the absence and in the presence of the DnaK system of cochaperones (Fig. 5, lane 8 versus lanes 4 and 6). As shown in Fig. 5, DnaK/DnaJ/GrpE decreased the amount of ClpB bound to aggregates, indicating that ClpB and DnaK

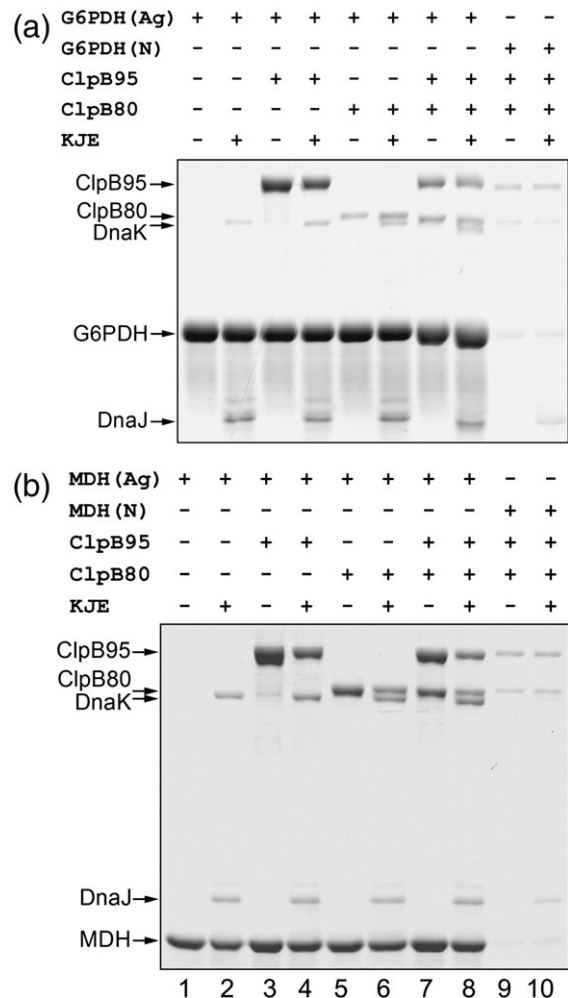


**Fig. 5.** Interactions of ClpB with aggregated substrates. Substrate-trapping variants of ClpB: ClpB95(E279Q/E678Q) and ClpB80(E279Q/E678Q) were incubated with native (N) or aggregated (Ag) G6PDH (a) or MDH (b) without or with DnaK/DnaJ/GrpE (KJE) in the presence of ATP (conditions as in Fig. 2). The solutions were passed through a 0.1- $\mu$ m filter. SDS-PAGE analysis with a Coomassie brilliant blue stain is shown for the fractions retained on the filter and subsequently solubilized with an SDS buffer. Representative results from three independent experiments are shown.

compete for substrate binding sites. Importantly, however, the excess chaperone activity of ClpB95/ClpB80 cannot be attributed to the aggregate binding capability.

Substrate translocation through the ClpB channel cannot be monitored directly, but it has been shown that in a related ATPase ClpX, the substrate translocation rate is tightly linked to the rate of ATP consumption.<sup>19</sup> We determined the ATP hydrolysis rates in mixtures of ClpB95 with ClpB80 (Fig. 6). In agreement with previous results,<sup>20</sup> the basal ATPase activity of ClpB80 (Fig. 6a) was higher than that of ClpB95, consistent with a higher propensity of ClpB80 to form oligomers (see Fig. 8). The basal ATPase activity of mixtures of ClpB95 with ClpB80 was approximately proportional to the ClpB80 fraction (Fig. 6a). This result is expected, as there is no difference between ClpB95 and ClpB80 within their AAA<sup>+</sup> modules.

It has been shown that model substrates of ClpB—a positively charged peptide B1 and  $\alpha$ -casein—are efficiently translocated through the ClpB channel even in the absence of cochaperones.<sup>8</sup> We found that the ATPase activity of ClpB95/ClpB80 is stimulated but remains approximately proportional to the

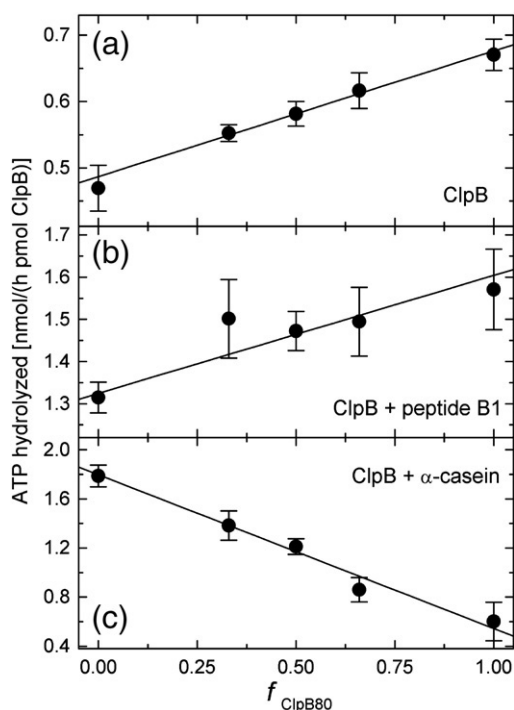


**Fig. 6.** ATPase activity of ClpB95 and ClpB80. The rate of ATP hydrolysis catalyzed by ClpB95 and ClpB80 was measured as a function of the molar fraction of ClpB80 ( $f_{\text{ClpB80}}$ ) without substrates (a), with 5  $\mu\text{M}$  peptide B1 (b), or with 0.2 mg/ml  $\alpha$ -casein (c). Inorganic phosphate production from ATP was determined in the presence of 25  $\mu\text{M}$  ClpB (a), 12  $\mu\text{M}$  ClpB (b), or 5  $\mu\text{M}$  ClpB (c) after 15 min at 37  $^{\circ}\text{C}$ . Mean values from six (a and c) or three (b) determinations are shown with standard deviations. Continuous lines illustrate linear regression fits of the experimental data.

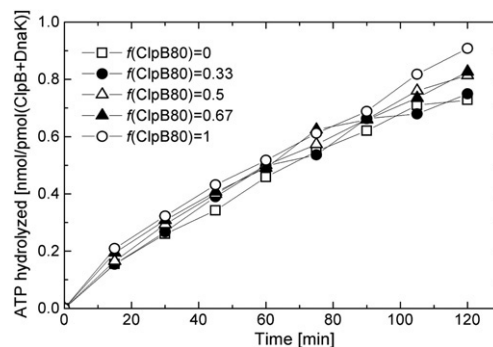


**Fig. 7.** ATP consumption by the ClpB-DnaK system during aggregate reactivation. Inorganic phosphate production was measured at indicated times during the reactivation of aggregated G6PDH (conditions as in Fig. 2a) with 1  $\mu\text{M}$  DnaK, 1  $\mu\text{M}$  DnaJ, 0.5  $\mu\text{M}$  GrpE (KJE) and 1.5  $\mu\text{M}$  ClpB95 (open squares), KJE with 1.5  $\mu\text{M}$  ClpB80 (open circles), KJE with 1  $\mu\text{M}$  ClpB95 and 0.5  $\mu\text{M}$  ClpB80 (filled circles), KJE with 0.75  $\mu\text{M}$  ClpB95 and 0.75  $\mu\text{M}$  ClpB80 (open triangles), or KJE with 0.5  $\mu\text{M}$  ClpB95 and 1  $\mu\text{M}$  ClpB80 (filled triangles).

ClpB80 fraction in the presence of peptide B1 or  $\alpha$ -casein (Fig. 6b and c). In the presence of  $\alpha$ -casein, the ATPase of ClpB80 is lower than that of ClpB95, showing that the N-terminal domain plays a role in  $\alpha$ -casein processing, as it does in reactivation of G6PDH (see Fig. 2). However, unlike chaperone activity, the ATPase of ClpB95/ClpB80 does not show any excess activation above the capabilities of both isolated isoforms. Moreover, no excess ATPase activity was observed during the reactivation of aggregated G6PDH by ClpB95/ClpB80 with DnaK/DnaJ/GrpE (Fig. 7) (i.e., under the conditions of Fig. 2a). This result indicates that the multichaperone system, including the ATPase DnaK and ClpB95 with ClpB80, does not utilize energy faster than that containing DnaK with only ClpB95 or only ClpB80. Nevertheless, ClpB95 and ClpB80 are more active in aggregate reactivation together than separately.

### ClpB95 and ClpB80 associate into hetero-oligomers

An excess chaperone activity of mixtures of ClpB95 with ClpB80 suggests that the two ClpB isoforms may physically interact. To detect hetero-association of ClpB95 and ClpB80, we investigated their association properties under conditions disfavoring homo-oligomer formation (i.e., at low protein concentration and in the absence of nucleotides). As shown in Fig. 8a, 5  $\mu\text{M}$  ClpB95 sedimented in an analytical ultracentrifuge as a monomeric  $\sim 4\text{S}$  particle, as also did 2.5  $\mu\text{M}$  ClpB80. However, when 5  $\mu\text{M}$  ClpB95 was combined with 2.5  $\mu\text{M}$  ClpB80, a significant population of  $\sim 13\text{S}$  oligomers was observed (Fig. 8b). From the area of the monomer and oligomer peaks, it can be estimated that  $\sim 40\%$  of ClpB is oligomeric under the conditions of Fig. 8b. Since none of the two isoforms formed homo-

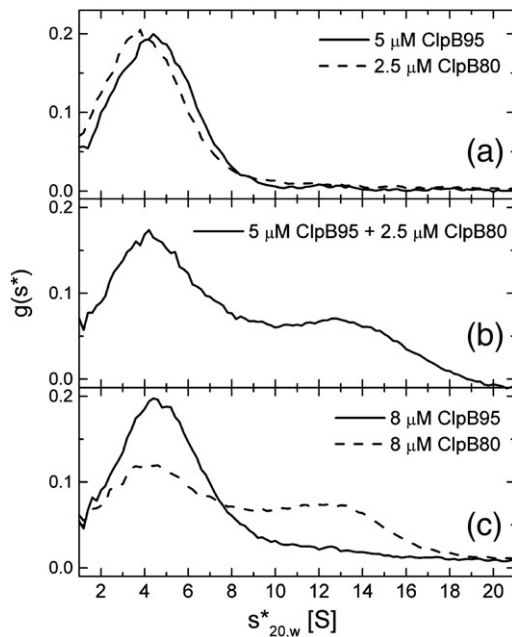


**Fig. 8.** Sedimentation velocity analysis of ClpB95 and ClpB80. Ultracentrifugation was performed at 50,000 rpm and 20 °C in 50 mM Tris-HCl (pH 7.5), 0.2 M KCl, 20 mM MgCl<sub>2</sub>, 1 mM EDTA, and 2 mM β-mercaptoethanol. Apparent sedimentation coefficient distributions  $g(s^*)$  versus  $s^*_{20,w}$  in Svedbergs (S) were calculated from time-dependent protein concentration profiles measured with absorption at 238 nm and are shown for 5 μM ClpB95 (a; continuous line), 2.5 μM ClpB80 (a; broken line), 5 μM ClpB95 with 2.5 μM ClpB80 (b), 8 μM ClpB95 (c; continuous line), and 8 μM ClpB80 (c; broken line).

oligomers at such protein concentration (Fig. 8a), the oligomers in Fig. 8b occur as a result of the interaction between ClpB95 and ClpB80 and represent hetero-oligomers of ClpB95 and ClpB80. In the experiment shown in Fig. 8b, the total ClpB concentration was 7.5 μM. As shown in Fig. 8c, ClpB95 at a similar concentration remained monomeric, but ClpB80 formed some homo-oligomers with a sedimentation coefficient similar to that of the hetero-oligomers shown in Fig. 8b.

In agreement with our previous results,<sup>20</sup> the self-association affinity of ClpB80 is higher than that of ClpB95 (Fig. 8c). Importantly, ClpB95 and ClpB80 form hetero-oligomers at concentrations that are too low to induce their homo-oligomerization (Fig. 8a and b). Moreover, the results in Fig. 8b and c demonstrate that interactions between ClpB95 and ClpB80 produce oligomers that are comparable in size to those formed by ClpB80 alone. Thus, ClpB95/ClpB80 interactions occur within a hexamer, not between hexameric ClpB95 and ClpB80. Since the difference in molecular weight between ClpB95 and ClpB80 is only ~16%, the resolution of sedimentation studies is not sufficient to determine the exact subunit composition of heterohexamers, nor it is possible to determine whether their population is homogeneous or heterogeneous.

## Discussion

In this work, we discovered that ClpB achieves its full potential as an aggregate-reactivating chaperone through the functional interaction of its two isoforms (see Figs. 2, 3, and 4). This result explains why the alternative translation initiation site in the ClpB gene has not been eliminated: *E. coli* produces two isoforms of ClpB to optimize the activity of this chaperone. We showed that ClpB80 plays an important role in ClpB function in spite of its lower intrinsic substrate binding capability. Within the family of AAA<sup>+</sup> ATPases, production of different-sized isoforms is not restricted to ClpB. A truncated isoform arising from the alternative translation initiation site was also found in ClpA, an ATPase component of the ClpAP protease.<sup>21</sup> Two different translation initiation sites are also used during production of spastin, a mammalian AAA<sup>+</sup> ATPase involved in microtubule severing.<sup>22</sup> Like in ClpB, the alternative N-termini in isoforms of AAA<sup>+</sup> ATPases are often located between the AAA<sup>+</sup> modules and distinct “attachment” domains. Since oligomeric ring formation is a common essential element of the mechanism of AAA<sup>+</sup> ATPases, our results raise a possibility that the functionality of other AAA<sup>+</sup> ATPases may be regulated by the production of multiple isoforms, their heteroassociation, and synergistic cooperation.

Where does the excess chaperone capability of ClpB95/ClpB80, which is absent in either ClpB95 or ClpB80, come from? The population of ClpB95+ClpB80 bound to aggregates is not significantly higher than that observed for each isolated isoform (see Fig. 5). This result indicates that the synergy is not linked to the aggregate binding capacity of ClpB. The rate of ATP hydrolysis catalyzed by ClpB95+ClpB80 is not faster than the sum of the rates produced by the isolated isoforms (see Figs. 6 and 7). This result suggests that the ATP-driven threading of substrates through the ClpB channel does not occur faster with ClpB95/ClpB80 than with the isolated isoforms. Altogether, our results indicate that another process in which the mixtures of ClpB95 with ClpB80 are superior to the isolated isoforms determines the overall rate of aggregate reactivation, as measured in Fig. 2.

We postulate that the rate-limiting step in aggregate reactivation occurs after ATP-stimulated substrate binding, which is represented in experiments with the substrate-trapping ClpB (see Fig. 5), and before substrate threading through the channel. Such a step, which has not been considered previously, might correspond to a commitment by ClpB to engage a structural element of a substrate with channel-located flexible loops<sup>23</sup> and may be a prerequisite to substrate translocation. It has been established that the N-terminal domain of ClpB and the channel loops interact with aggregated substrates,<sup>12,24</sup> but it is not known whether these two sites in ClpB interact with the same part of the aggregate. It is possible that the unique N-terminal



domain allows ClpB to distinguish between aggregated and nonaggregated proteins, whereas the channel loops (whose sequence in ClpB is similar to that of other AAA<sup>+</sup> ATPases) drive polypeptide translocation. The commitment step may be rate-controlling because the lifetime of surface-exposed motifs that can be efficiently extracted by the channel loops may be limited. Our results indicate that functional interaction between ClpB95 and ClpB80 does not enhance the overall substrate binding capability or the rate of ATP-driven substrate extraction, but it may optimize the probability of matching ClpB with extractable structural elements.

Ring-like AAA<sup>+</sup> oligomers are stabilized by extensive contacts between wedge-shaped AAA<sup>+</sup> modules.<sup>25</sup> Mutual association of ClpB95 and ClpB80 (see Fig. 8) is not surprising, since both isoforms contain identical AAA<sup>+</sup> modules and differ only in the N-terminal region. Indeed, interaction between ClpB95 and ClpB80 has been observed before by Kim *et al.*<sup>14</sup> Unexpectedly, we discovered that ClpB95/ClpB80 heterohexamers form preferentially over ClpB95 homohexamers (Fig. 8). Thus, when ClpB95 and ClpB80 are produced *in vivo* or combined *in vitro*, they can be expected to associate into homohexamers, as well as into heterohexamers, whose population would depend on the concentrations and molar ratio of the two isoforms. It is tempting to link the hetero-oligomerization of ClpB95 and ClpB80 with the excess chaperone activity of ClpB95/ClpB80 (see Figs. 2, 3, and 4). However, to unequivocally prove that the hetero-oligomers are responsible for the excess activity, we should produce modified variants of ClpB95 and ClpB80 that form only homo-oligomers, but not hetero-oligomers. Because the AAA<sup>+</sup> modules that mediate oligomerization are identical in ClpB95 and ClpB80, the production of such “negative-control” protein variants is virtually impossible.

Alternatively, the synergy between ClpB95 and ClpB80 might arise from the interaction between homohexameric ClpB95 and ClpB80, which might activate each other during substrate reactivation. Although such mechanism cannot be disproven by our results, we consider it less likely because no interaction between ClpB hexamers has been detected in previous studies<sup>6,26</sup> and, importantly, hexamers are the largest oligomers detected when ClpB95 is mixed with ClpB80 (see Fig. 8).

Why would the hetero-oligomers of ClpB95 with ClpB80 form preferentially over the homo-oligomers of ClpB95 (see Fig. 8)? Analogous preferential hetero-oligomerization of two different AAA<sup>+</sup> helicases, Rvb1 and Rvb2, has been observed before.<sup>27</sup> Interestingly, as in the case of ClpB95/ClpB80, the activity of Rvb1/Rvb2 is higher than that of the isolated components.<sup>27</sup>

Results shown in Fig. 8 imply that formation of a full ring of the N-terminal domains in a hexameric ClpB is thermodynamically unfavorable, as compared to rings without some or all N-terminal

domains. The “penalty” for forming a ring of the N-terminal domains may be due to an unfavorable enthalpy (steric repulsion) and/or an unfavorable entropy (restriction of mobility). Indeed, a high mobility of the N-terminal domain in a nonphysiological incomplete ClpB oligomer has been shown by the crystal structure.<sup>5</sup> We used a structural model of the hexameric ClpB from *Thermus thermophilus*<sup>28</sup> to compute and compare the mobility of the N-terminal domain in a homohexamer of ClpB95 and in a heterohexamer with three ClpB95 and three ClpB80 subunits. Figure 9 shows the results of the elastic normal-mode analysis<sup>29</sup> of large-scale correlated motions in ClpB hexamers. In the homohexamer of ClpB95 (Fig. 9a, broken line; Fig. 9b), the normal-mode analysis detects the high mobility of two regions located outside of the ClpB ring: the tip of the coiled-coil middle domain (residues 400–450) and the C-terminal subdomain of the D2 AAA<sup>+</sup> module (residues 750–854). The D2 subdomain maintains the stability of the ring,<sup>20</sup> while the coiled-coil middle domain supports the chaperone activity of ClpB by an unknown mechanism.<sup>5,30</sup> In the ClpB95/ClpB80 heterohexamer (Fig. 9a, continuous line; Fig. 9c), a third mobile structural region (residues 1–140) that corresponds to the N-terminal domain has been detected (see Fig. 1). The mobility of the N-terminal domain is suppressed in the ClpB95 homohexamer. This result indicates that the excess thermodynamic stability of the ClpB95/ClpB80 heterohexamers with an incomplete N-terminal ring may arise from elimination of entropic penalty due to restriction of the mobility of the N-terminal domains. Furthermore, one can speculate that the enhanced mobility of the N-terminal domain in the ClpB95/ClpB80 hetero-oligomers may support the efficient matching of the extractable motifs with the conformation of the channel loops and produce higher rates of substrate disaggregation with ClpB95/ClpB80 than with ClpB95 (see Figs. 2, 3, and 4).

Whereas some aggregates, notably small ones, can be reactivated by DnaK/DnaJ/GrpE, the reactivation of larger aggregates requires ClpB.<sup>31</sup> Preincubation of aggregates with DnaK accelerates their subsequent reactivation with ClpB.<sup>32</sup> DnaK and DnaJ (but not the nucleotide exchange factor GrpE) are found in complex with aggregated proteins (see Fig. 5). Importantly, direct interaction of DnaK or DnaJ with ClpB has been ruled out in previous studies.<sup>33</sup> We found that binding of ClpB to aggregates does not require DnaK (Fig. 5). Importantly, DnaK does not increase the population of ClpB bound to the aggregates; conversely, it competes with ClpB in aggregate binding (see Fig. 5). These results are inconsistent with a recent model suggesting that DnaK disaggregates substrates before they are transferred to ClpB.<sup>34</sup> It can be rather proposed that DnaK might reversibly interact with aggregates and modify their surface to expose ClpB-extractable motifs. Thus, the activity of DnaK and the synergy between two ClpB isoforms might produce a similar effect: facilitate a commitment by

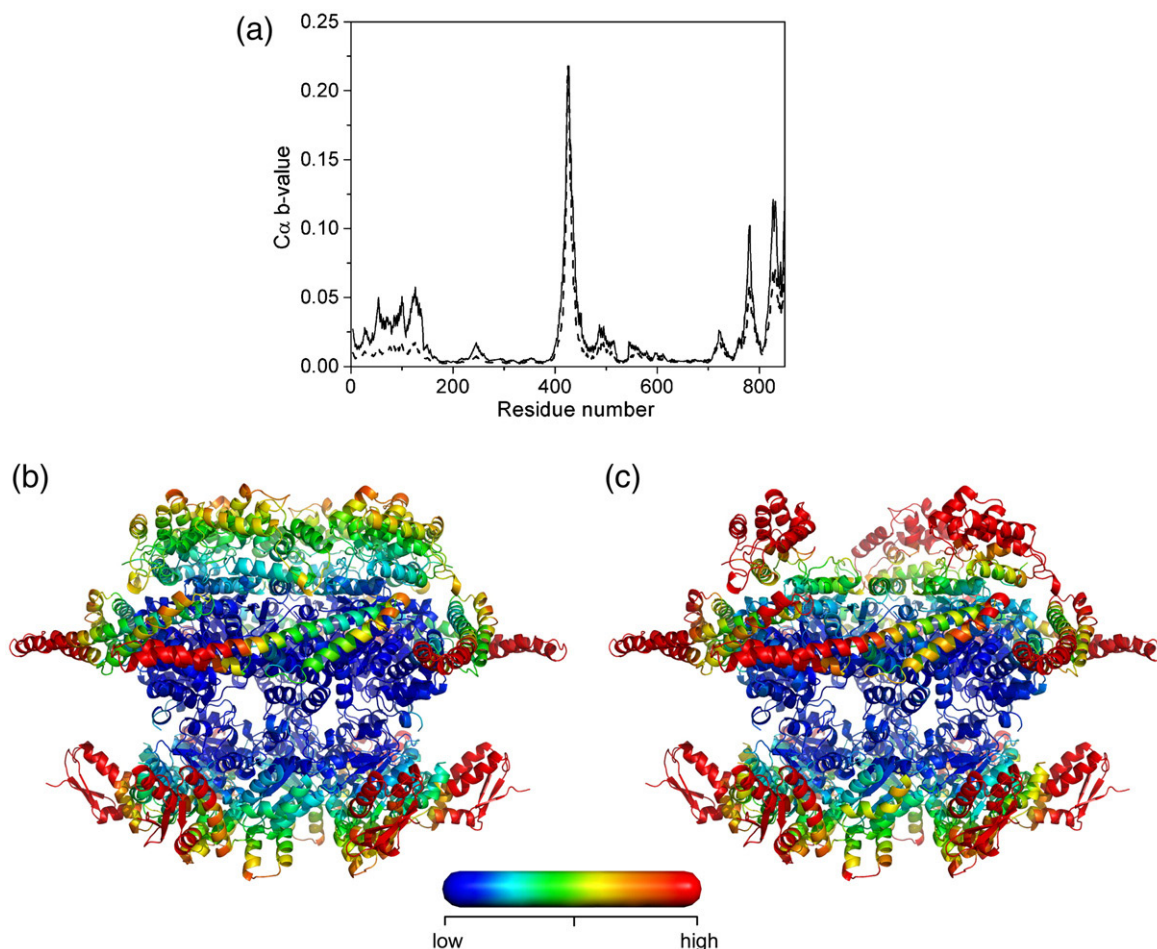


**Fig. 9.** Normal-mode analysis of main-chain mobility in hexameric ClpB. Elastic normal-mode analysis was performed with the hexameric models of *T. thermophilus* ClpB<sup>28</sup> containing either six full-length ClpB95 subunits [a (broken line) and b] or three ClpB95 and three ClpB80 subunits [a (continuous line) and c]. In (a), the values of  $\alpha$ -carbon *B*-factors calculated from the first 100 oscillatory normal modes are shown for each residue in the sequence of a ClpB95. The hexamer side views in (b) and (c) are color-coded according to the values of *B*-factor (dark blue: lowest *B*-factor; red: highest *B*-factor). The N-terminal domain is on top of the structures shown in (b) and (c). For clarity of presentation, the color scale maximum has been selected to correspond to the highest *B*-factor within the N-terminal domain of ClpB95.

ClpB to extract polypeptides from the aggregates and accelerate aggregate reactivation.

## Materials and Methods

### Proteins and aggregates

Chaperones were produced or obtained as previously described.<sup>12</sup> G6PDH from *Leuconostoc mesenteroides* and  $\alpha$ -casein were obtained from Sigma (St. Louis, MO). Porcine heart MDH was obtained from MP Biomedicals (Irvine, CA). Protein concentrations were determined spectrophotometrically and are given in monomer units. To prepare large aggregates of G6PDH, we incubated urea-denatured 220  $\mu$ M G6PDH<sup>12</sup> at 47 °C for 5 min, diluted it 10-fold in buffer A [50 mM triethanolamine/Cl (pH 7.5), 20 mM Mg(OAc)<sub>2</sub>, 30 mM KCl, 1 mM  $\beta$ -mercaptoethanol, and 1 mM ethylenediaminetetraacetic acid (EDTA)], and incubated it at 47 °C for 15 min and then on ice for 2 min. To prepare aggregated MDH, we diluted a 250  $\mu$ M stock solution 20-fold in buffer B [100 mM Tris (pH 7.5), 120 mM KCl, 15 mM Mg(OAc)<sub>2</sub>, and 8 mM DTT] and incubated it at

47 °C for 60 min. The solution was then mixed and incubated on ice for 2 min. Immunodetection of ClpB was performed with rabbit polyclonal anti-ClpB antibodies.<sup>35</sup> Peptide B1 (AHAWQHQQGKTLFISRKT<sup>24</sup>) was produced by the KSU Biotechnology Core Facility and purified with reversed-phase chromatography.

### Bacterial strains and plasmids

*E. coli* MC4100 (SG20250) [*araD139*,  $\Delta$ (*argF-lac*)U169, *rpsL150*, *relA1*, *deoC1*, *ptsF25*, *rpsR*, *flbB5301*] was obtained from S. Gottesman (National Cancer Institute, Bethesda, MD), and MC4100  $\Delta$ *clpB*:kan was supplied by A. Toussaint (Université Libre de Bruxelles, Brussels, Belgium). Plasmid pQF70 containing the *luxAB* (luciferase) genes from *Vibrio harveyi*<sup>36</sup> was obtained from M. Kropinski (Queen's University, Kingston, Ontario, Canada) via H. Pan-Hou (Setsunan University, Osaka, Japan). Plasmid pHSG-luci carrying the *Photinus pyralis* luciferase gene was a gift from A. Mogk (ZMBH, Heidelberg, Germany). Plasmid pClpB7 (here designated as pClpB95/ClpB80) carrying the entire *clpB* gene of *E. coli* together with the  $\sigma^{32}$ -dependent promoter was constructed as described previously.<sup>37</sup> Plasmid pBS-ClpB93 containing *clpB95* was



obtained from C. -H. Chung (Seoul National University, Seoul, Korea). To construct a plasmid pClpB80, we amplified the 415-bp XmaI/VspI fragment carrying the  $\sigma^{32}$  promoter of *clpB* and the 2129-bp VspI/PstI fragment containing a sequence of ClpB80 by PCR from pClpB7 and inserted them into the low-copy-number plasmid pGB2 (spc<sup>R</sup> and str<sup>R</sup>) that had been precut with XmaI/PstI. In the final plasmid product, the GUG codon at the N-terminus of ClpB80 was replaced by AUG. Plasmid pClpB95 expressing ClpB95 was constructed by amplification of the entire *clpB* gene together with the  $\sigma^{32}$  promoter from pBS-ClpB93<sup>38</sup> and then by subcloning into the XmaI and PstI sites of pGB2. The *luxAB* genes were amplified by PCR from pQF70 and cloned into the BamHI and HindIII sites of pHSG-luciferase, replacing the *P. pyralis* luciferase gene. The final recombinant plasmid was designated as pLucVh.

### In vitro protein reactivation assays

Aggregates of G6PDH were diluted to 3  $\mu$ M in buffer A with 6 mM ATP containing either no chaperone, 1  $\mu$ M DnaK, 1  $\mu$ M DnaJ and 0.5  $\mu$ M GrpE (KJE) with 1.5  $\mu$ M ClpB95, KJE with 1.5  $\mu$ M ClpB80, or KJE with mixtures of ClpB95 and ClpB80 (total of 1.5  $\mu$ M ClpB). Aggregates of MDH were diluted to 3  $\mu$ M in buffer B with 6 mM ATP containing either no chaperone or KJE with ClpB95 and/or ClpB80 (concentrations as described above). After incubation at 30 °C, aliquots were withdrawn, and G6PDH or MDH activity was measured.

### Enzymatic assays

G6PDH samples were incubated at 30 °C in 50 mM Tris-HCl (pH 7.8) and 5 mM MgCl<sub>2</sub> with 2 mM glucose-6-phosphate and 1 mM NADP<sup>+</sup>. Absorption at 340 nm was measured after 5 min. MDH samples were incubated at 25 °C in 50 mM Tris-HCl (pH 7.4), 2 mM DTT, 0.3 mM oxaloacetate, and 0.15 mM NADH. Absorption at 340 nm was measured after 20 min. ATPase activity was measured as described before.<sup>2</sup>

### In vivo reactivation assays

Cultures of *E. coli* MC4100 $\Delta$ *clpB* producing luciferase and carrying either pGB2 (control), pClpB95/ClpB80, pClpB95, or pClpB80 were grown in LB at 30 °C to an OD<sub>600</sub> of 0.5. Expression of luciferase genes was induced with 1 mM IPTG for 1 h at 30 °C. For thermal inactivation, the culture producing *P. pyralis* luciferase was incubated for 15 min at 45 °C, and the culture producing *V. harveyi* luciferase was incubated for 25 min at 45 °C, both in the presence of tetracycline (25  $\mu$ g/ml) to block *de novo* protein synthesis. Culture recovery was monitored by further incubation at 30 °C for 90–120 min. *P. pyralis* luciferase activity was determined with the Luciferase Assay System (Promega). For *V. harveyi* luciferase assay, 200- $\mu$ l culture aliquots were withdrawn at the indicated times and mixed with 7  $\mu$ l of 10% *n*-decanal in ethanol for up to 1 min. Luminescence produced by the luciferases was monitored using a Berthold luminometer.

### Determination of cellular aggregate content

Cells were fractionated by sucrose-density gradient ultracentrifugation, as described before.<sup>15,39</sup> Briefly, the cells were gently lysed, layered on a two-step sucrose density gradient (1 ml of 55% and 5 ml of 17% wt/wt

sucrose in 3 mM EDTA, pH 7.6), and centrifuged for 90 min in a Beckman SW41 Ti rotor at 240,000g. One-milliliter CP subfraction (cytoplasmic and periplasmic proteins) was collected from the top of the gradient, and 1 ml of membrane fractions also containing the heat-aggregated proteins was collected from the bottom. Membrane/aggregate fractions were further separated in a five-step density gradient: 55% (1.4 ml), 50%, 45%, 40% (2.3 ml of each), and 35% (1.4 ml) sucrose in 3 mM EDTA (pH 7.6). After centrifugation in a Beckman SW41 Ti rotor at 240,000g for 16 h, 400- $\mu$ l fractions containing the aggregates were collected from the bottom, and protein concentration was measured by the Bradford method with serum albumin as standard.

### ClpB–aggregate interaction assay

Native or aggregated G6PDH (3  $\mu$ M) or MDH (3  $\mu$ M) was shaken for 5 min at 30 °C in buffer A or B, respectively, with 5 mM ATP and 1.5  $\mu$ M ClpB95(E279Q/E678Q), 1.5  $\mu$ M ClpB80(E279Q/E678Q), or a 1:1 mixture of ClpB95(E279Q/E678Q) and ClpB80(E279Q/E678Q) (total of 1.5  $\mu$ M ClpB) without or with 1  $\mu$ M DnaK, 1  $\mu$ M DnaJ, and 0.5  $\mu$ M GrpE. Seventy-five-microliter aliquots were applied to Amicon Ultrafree-MC centrifugal filter devices with a 0.1- $\mu$ m Durapore membrane (Millipore). Filter units were incubated for 3 min at room temperature and then centrifuged for 4 min at 12,000g. The filters were washed with buffer A or B containing 5 mM ATP. Proteins retained on the membrane were eluted by 10-min incubation at 47 °C with 75  $\mu$ l of SDS sample buffer and centrifugation (4 min at 12,000g). Eluates were analyzed by SDS-PAGE and Coomassie brilliant blue staining.

### Analytical ultracentrifugation

Beckman XL-I analytical ultracentrifuge was used in sedimentation velocity experiments at 50,000 rpm and 20 °C with two-channel aluminum analytical cells. ClpB solutions were prepared in 50 mM Tris-HCl (pH 7.5), 0.2 M KCl, 20 mM MgCl<sub>2</sub>, 1 mM EDTA, and 2 mM  $\beta$ -mercaptoethanol. ClpB95 and ClpB80 were diluted to the desired concentrations and mixed before being loaded into the centrifuge cell. The data were analyzed using the time-derivative method<sup>40</sup> and the software distributed with the instrument.

### Normal-mode analysis

We used Protein Data Bank coordinates of the hexameric model of the full-length *T. thermophilus* ClpB.<sup>28</sup> The ElNemo web server<sup>†</sup><sup>29</sup> was used to compute the *B*-factor for each residue based on the first 100 normal modes. One computation was performed on the hexamer composed of six full-length ClpB95 chains. In another computation, the hexamer was composed of three full-length chains (A, C, and E) and three truncated ones (B, D, and F), with the N-terminal domain removed (residues 4–139).

## Acknowledgements

This work was supported by the National Institutes of Health (GM58626), the Polish Committee for

<sup>†</sup> <http://www.igs.cnrs-mrs.fr/elNemo/>

Scientific Research (0668/P01/2006/30), Terry C. Johnson Center for Basic Cancer Research, and the Kansas Agricultural Experiment Station (contribution 06-158-J).

## References

- Glover, J. R. & Lindquist, S. (1998). Hsp104, Hsp70, and Hsp40: a novel chaperone system that rescues previously aggregated proteins. *Cell*, **94**, 73–82.
- Zolkiewski, M. (1999). ClpB cooperates with DnaK, DnaJ, and GrpE in suppressing protein aggregation. A novel multi-chaperone system from *Escherichia coli*. *J. Biol. Chem.* **274**, 28083–28086.
- Goloubinoff, P., Mogk, A., Zvi, A. P., Tomoyasu, T. & Bukau, B. (1999). Sequential mechanism of solubilization and refolding of stable protein aggregates by a bichaperone network. *Proc. Natl Acad. Sci. USA*, **96**, 13732–13737.
- Neuwald, A. F., Aravind, L., Spouge, J. L. & Koonin, E. V. (1999). AAA<sup>+</sup>: a class of chaperone-like ATPases associated with the assembly, operation, and disassembly of protein complexes. *Genome Res.* **9**, 27–43.
- Lee, S., Sowa, M. E., Watanabe, Y. H., Sigler, P. B., Chiu, W., Yoshida, M. & Tsai, F. T. (2003). The structure of ClpB: a molecular chaperone that rescues proteins from an aggregated state. *Cell*, **115**, 229–240.
- Akoev, V., Gogol, E. P., Barnett, M. E. & Zolkiewski, M. (2004). Nucleotide-induced switch in oligomerization of the AAA<sup>+</sup> ATPase ClpB. *Protein Sci.* **13**, 567–574.
- Haslberger, T., Zdanowicz, A., Brand, I., Kirstein, J., Turgay, K., Mogk, A. & Bukau, B. (2008). Protein disaggregation by the AAA<sup>+</sup> chaperone ClpB involves partial threading of looped polypeptide segments. *Nat. Struct. Mol. Biol.* **15**, 641–650.
- Weibezahn, J., Tessarz, P., Schlieker, C., Zahn, R., Maglica, Z. & Lee, S. (2004). Thermotolerance requires refolding of aggregated proteins by substrate translocation through the central pore of ClpB. *Cell*, **119**, 653–665.
- Doyle, S. M., Shorter, J., Zolkiewski, M., Hoskins, J. R., Lindquist, S. & Wickner, S. (2007). Asymmetric deceleration of ClpB or Hsp104 ATPase activity unleashes protein-remodeling activity. *Nat. Struct. Mol. Biol.* **14**, 114–122.
- Woo, K. M., Kim, K. I., Goldberg, A. L., Ha, D. B. & Chung, C. H. (1992). The heat-shock protein ClpB in *Escherichia coli* is a protein-activated ATPase. *J. Biol. Chem.* **267**, 20429–20434.
- Chow, I. T. & Baneyx, F. (2005). Coordinated synthesis of the two ClpB isoforms improves the ability of *Escherichia coli* to survive thermal stress. *FEBS Lett.* **579**, 4235–4241.
- Barnett, M. E., Nagy, M., Kedzierska, S. & Zolkiewski, M. (2005). The amino-terminal domain of ClpB supports binding to strongly aggregated proteins. *J. Biol. Chem.* **280**, 34940–34945.
- Chow, I. T., Barnett, M. E., Zolkiewski, M. & Baneyx, F. (2005). The N-terminal domain of *Escherichia coli* ClpB enhances chaperone function. *FEBS Lett.* **579**, 4242–4248.
- Kim, K. I., Cheong, G. W., Park, S. C., Ha, J. S., Woo, K. M., Choi, S. J. & Chung, C. H. (2000). Heptameric ring structure of the heat-shock protein ClpB, a protein-activated ATPase in *Escherichia coli*. *J. Mol. Biol.* **303**, 655–666.
- Kucharczyk, K., Laskowska, E. & Taylor, A. (1991). Response of *Escherichia coli* cell membranes to induction of lambda cl857 prophage by heat shock. *Mol. Microbiol.* **5**, 2935–2945.
- Tomoyasu, T., Mogk, A., Langen, H., Goloubinoff, P. & Bukau, B. (2001). Genetic dissection of the roles of chaperones and proteases in protein folding and degradation in the *Escherichia coli* cytosol. *Mol. Microbiol.* **40**, 397–413.
- Weibezahn, J., Schlieker, C., Bukau, B. & Mogk, A. (2003). Characterization of a trap mutant of the AAA<sup>+</sup> chaperone ClpB. *J. Biol. Chem.* **278**, 32608–32617.
- Nagy, M., Wu, H. C., Liu, Z., Kedzierska-Mieszkowska, S. & Zolkiewski, M. (2009). Walker-A threonine couples nucleotide occupancy with the chaperone activity of the AAA<sup>+</sup> ATPase ClpB. *Protein Sci.* **18**, 287–293.
- Kenniston, J. A., Baker, T. A., Fernandez, J. M. & Sauer, R. T. (2003). Linkage between ATP consumption and mechanical unfolding during the protein processing reactions of an AAA<sup>+</sup> degradation machine. *Cell*, **114**, 511–520.
- Barnett, M. E., Zolkiewska, A. & Zolkiewski, M. (2000). Structure and activity of ClpB from *Escherichia coli*. Role of the amino- and -carboxyl-terminal domains. *J. Biol. Chem.* **275**, 37565–37571.
- Seol, J. H., Yoo, S. J., Kim, K. I., Kang, M. S., Ha, D. B. & Chung, C. H. (1994). The 65-kDa protein derived from the internal translational initiation site of the clpA gene inhibits the ATP-dependent protease Ti in *Escherichia coli*. *J. Biol. Chem.* **269**, 29468–29473.
- Claudian, P., Riano, E., Errico, A., Andolfi, G. & Rugarli, E. I. (2005). Spastin subcellular localization is regulated through usage of different translation start sites and active export from the nucleus. *Exp. Cell Res.* **309**, 358–369.
- Hinnerwisch, J., Fenton, W. A., Furtak, K. J., Farr, G. W. & Horwich, A. L. (2005). Loops in the central channel of ClpA chaperone mediate protein binding, unfolding, and translocation. *Cell*, **121**, 1029–1041.
- Schlieker, C., Weibezahn, J., Patzelt, H., Tessarz, P., Strub, C. & Zeth, K. (2004). Substrate recognition by the AAA<sup>+</sup> chaperone ClpB. *Nat. Struct. Mol. Biol.* **11**, 607–615.
- Ogura, T. & Wilkinson, A. J. (2001). AAA<sup>+</sup> superfamily ATPases: common structure–diverse function. *Genes Cells*, **6**, 575–597.
- Zolkiewski, M., Kessel, M., Ginsburg, A. & Maurizi, M. R. (1999). Nucleotide-dependent oligomerization of ClpB from *Escherichia coli*. *Protein Sci.* **8**, 1899–1903.
- Gribun, A., Cheung, K. L., Huen, J., Ortega, J. & Houry, W. A. (2008). Yeast Rvb1 and Rvb2 are ATP-dependent DNA helicases that form a heterohexameric complex. *J. Mol. Biol.* **376**, 1320–1333.
- Diemand, A. V. & Lupas, A. N. (2006). Modeling AAA<sup>+</sup> ring complexes from monomeric structures. *J. Struct. Biol.* **156**, 230–243.
- Suhre, K. & Sanejouand, Y. H. (2004). ElNemo: a normal mode Web server for protein movement analysis and the generation of templates for molecular replacement. *Nucleic Acids Res.* **32**, W610–W614.
- Haslberger, T., Weibezahn, J., Zahn, R., Lee, S., Tsai, F. T., Bukau, B. & Mogk, A. (2007). M domains couple the ClpB threading motor with the DnaK chaperone activity. *Mol. Cell*, **25**, 247–260.
- Diamant, S., Ben Zvi, A. P., Bukau, B. & Goloubinoff, P. (2000). Size-dependent disaggregation of stable protein aggregates by the DnaK chaperone machinery. *J. Biol. Chem.* **275**, 21107–21113.

32. Zietkiewicz, S., Krzewska, J. & Liberek, K. (2004). Successive and synergistic action of the Hsp70 and Hsp100 chaperones in protein disaggregation. *J. Biol. Chem.* **279**, 44376–44383.
33. Kedzierska, S., Chesnokova, L. S., Witt, S. N. & Zolkiewski, M. (2005). Interactions within the ClpB/DnaK bi-chaperone system from *Escherichia coli*. *Arch. Biochem. Biophys.* **444**, 61–65.
34. Zietkiewicz, S., Lewandowska, A., Stocki, P. & Liberek, K. (2006). Hsp70 chaperone machine remodels protein aggregates at the initial step of Hsp70–Hsp100-dependent disaggregation. *J. Biol. Chem.* **281**, 7022–7029.
35. Tek, V. & Zolkiewski, M. (2002). Stability and interactions of the amino-terminal domain of ClpB from *Escherichia coli*. *Protein Sci.* **11**, 1192–1198.
36. Farinha, M. A. & Kropinski, A. M. (1990). Construction of broad-host-range plasmid vectors for easy visible selection and analysis of promoters. *J. Bacteriol.* **172**, 3496–3499.
37. Kedzierska, S., Akoev, V., Barnett, M. E. & Zolkiewski, M. (2003). Structure and function of the middle domain of ClpB from *Escherichia coli*. *Biochemistry*, **42**, 14242–14248.
38. Park, S. K., Kim, K. I., Woo, K. M., Seol, J. H., Tanaka, K. & Ichihara, A. (1993). Site-directed mutagenesis of the dual translational initiation sites of the *clpB* gene of *Escherichia coli* and characterization of its gene products. *J. Biol. Chem.* **268**, 20170–20174.
39. Kedzierska, S., Staniszevska, M., Wegrzyn, A. & Taylor, A. (1999). The role of DnaK/DnaJ and GroEL/GroES systems in the removal of endogenous proteins aggregated by heat-shock from *Escherichia coli* cells. *FEBS Lett.* **446**, 331–337.
40. Stafford, W. F., III (1992). Boundary analysis in sedimentation transport experiments: a procedure for obtaining sedimentation coefficient distributions using the time derivative of the concentration profile. *Anal. Biochem.* **203**, 295–301.